Influence of Long-Range Interactions on Diffusion Behavior in Semidilute Solution: Dynamics of Cellulose Diacetate in Quiescent State

Yoshisuke Tsunashima,* Hiroyuki Kawanishi, Ryosuke Nomura, and Fumitaka Horii

Institute for Chemical Research, Kyoto University, Uji, Kyoto 611-0011, Japan

Received February 16, 1999; Revised Manuscript Received June 7, 1999

ABSTRACT: The dynamics of cellulose diacetate (CDA) in semidilute solution ($1.4c^* < c < 5c^*$) was investigated in a *good* and high-polarity solvent, dimethylacetamide (DMAc), by dynamic light scattering in the quiescent state at 30 °C. Two fast diffusion motions and a very slow diffusion motion were detected, all the behavior of which is not expected from the framework of dynamics for usual flexible polymers in good solvents. The fast (fast mode) and medium-fast (medium mode) motions gave the diffusion coefficients D_F and D_M as $D_F \propto c^{0.40}$ and $D_M \propto c^{0.55}$. Both were the cooperative diffusion motions, or the relaxations of concentration fluctuations in two types of coarse-dense structures, which were realized as a nest of structures in a dynamic sense in semidilute solution. However, the relaxation rates were suppressed by the long-ranged hydrogen-bond interaction between hydroxyl (OH) groups on CDA molecules, and the interactions brought the systems into the *medium*, not good, solvent state. The slow diffusion (slow mode), which showed $D_S \propto c^{-2.44}$, could be described as a self-diffusion, where the semiflexible CDA chain performs the reptation in a virtual tube that was constructed by other surrounding CDA chains. The reptation motion would be retarded, much more than neutral flexible chains, by the chain stiffness and by the attractive long-ranged hydrogen-bond interaction operating OH groups between the reptating CDA chain and the tube wall.

Introduction

Cellulose diacetate (CDA) is the derivative of cellulose, one of the plant structural polysaccharides. Its chemical structure is given by Figure 1: Two of three hydroxyl (OH) groups at the C-2, 3, and 6 positions of each glucose residue on cellulose are substituted *on average* by OR with R the acetyl ($COCH_3$) group; that is, the *total* degree of substitution, DS, is about 2. Its conformational properties in various solvents depend strongly on both the *individual* DS for three OH groups on each glucose unit (i.e., how many and which of the three C-2, 3, and 6 position OH groups are substituted by OR?) and the sequential distribution of the glucose units with different individual DS along the chain, as well as on the total DS.[1] It is thus expected that CDA forms clusters in solvents of high polarity (or electronegativity), and the clusters will appear as steady stable associations or as temporally and locally induced increases in the solute mass concentration. Long-range interactions such as the hydrogen bond, which acts between intra- or intermolecular OH groups directly or via polar solvents, enhances a possibility that CDA takes various structures depending on solvents, temperature, imposed external fields, polymer mass concentration, and so forth. In fact, in the quiescent dilute solution of CDA in *N*,*N*-dimethylacetamide (DMAc, good solvent for CDA with the dipole moment $\mu = 3.72$ D) at 30 °C, we have observed that CDA took semiflexible-chain nature of the persistence length 8.0 nm[1] and showed two extra modes of motion in dynamics,[2] which could never be observed in usual polymer/solvent systems in dilute solution.[3] In other words, two relaxations of concentration fluctuations appear in dilute solution and coexist with the translational, or the center-of-mass, diffusion of the single CDA molecule. These two concentration fluctuations are found to be created by a nested mechanism of the creation−dissipation processes of locally but temporarily clustered CDA molecules in dilute solution with the help of the hydrogen bonding between OH groups of CDA in DMAc.[2]

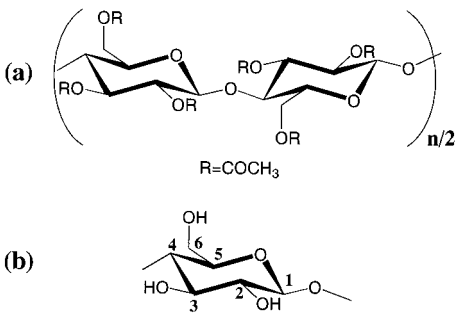

Figure 1. Chemical structures of (a) cellulose acetates (CA) and (b) the repeating unit, glucose residue. The three hydroxyl groups at C-2, 3, and 6 positions of a glucose residue on cellulose are substituted partly or fully by OR. Here R represents the acetyl groups (−$COCH_3$). For usual CA, the position and the number of substitution (or the degree of substitution, DS) in each glucose residue are not controlled. CDA is the general term for CA with DS = 2−2.5 on average, regardless of the microstructure on substitution.

In semidilute solution where polymer chains begin to overlap each other, usual neutral polymers have been expected from the scaling theory[4,5] to show two types of diffusion motion in good solvents, the fast one being the cooperative diffusion due to the relaxation of local concentration fluctuations to the level of the bulk concentration c and the slow one the self-diffusion (or reptation) of a single chain passing through the quasi-network made by entangled chains. When no specific interaction such as long-range interactions works be-

* To whom correspondences should be addressed.

10.1021/ma9902145 CCC: $18.00
Published on Web 07/23/1999

tween chains, the fast diffusion coefficient D_{coop} gives the positive dependence on concentration $D_{coop} \propto c^{\alpha}M^{0}$ and the slow one the negative one $D_{self} \propto c^{\beta}M^{-2}$ with $\alpha = {}^3/_4$ and $\beta = -{}^7/_4$, respectively, in good solvents.[4,5] In dynamic light scattering (DLS) experiments, two modes of diffusion motions have been observed for usual polymers,[6−15] though not always being assigned to the modes predicted from the scaling arguments. Moreover, the scaling exponents ${}^3/_4$ and $-{}^7/_4$ were found to be achieved only in a very limited range of c, M, and solvent quality with the experimental results that $\alpha = 0.4-0.77$ for PS in good solvents.[6−10,13−15] The proposal of the marginal solvent region was thus made[16] and verified,[11,16] which gave $\alpha = {}^1/_2$. For the slow mode, another concept different from the reptation, that is, the relaxation of transient clusters of loosely entangled chains,[17−19] has been proposed with β close to or steeper than -1.75 for poly(ethylene oxide),[17] poly(vinylpyrrolidone),[18] and PMMA.[19] Gelatin[20,21] and polynucleotides (polyadenilic acid)[22] in aqueous solution showed also the slow mode as self-diffusion or structural relaxations. Special attention should be paid to recent works on polysaccharides in solution.[23−25] In semidilute solution of all these samples, slow modes have been reported with β much steeper than -1.75, i.e., $\beta = -2.86$ for cellulose tricarbanilate (CTC) in dioxane,[23] $\beta = -2.56$ for cellulose tri-3-chlorophenylcarbamate (CT-3Cl-C) in dioxane,[24] and $\beta = -1.85$ and -6.9 for starch fractions in 0.5 N NaOH.[25] The first two samples belong to the derivatives of plant structural polysaccharides, and the last one belongs to plant reserve polysaccharides. The structural formation of these polysaccharides would be strongly influenced by long-range interactions exerted in solution. Thus, it can be expected that long-range interactions will induce drastic changes in dynamic feature of polymer chains in semidilute solution since such interactions will work more effectively than the case in dilute solution. As described already,[1,2] CDA showed even in dilute solution the unique dynamic feature that contains (i) the translational diffusion of a CDA molecule and (ii) two cooperative diffusions due to the concentration fluctuations accompanied by the process of local and temporal association−dissipation of CDA. No such singularity has been observed in CTC, CT-3Cl-C, and starch in dilute solution,[23−25] probably because of lacking in OH groups on these chains. It is very interesting to investigate the dynamic feature of CDA in semidilute solution—how the tentative structures in dilute solution will develop with the increase of polymer concentration and disclose specific behavior. In this work, we measured by DLS the dynamics of CDA in DMAc in the quiescent semidilute solution and discussed the effect of long-range interactions on the formation and the nature of dynamic structures of CDA in a high-polarity solvent DMAc.

Experimental Section

Materials and Solution Preparation. The CDA sample used was Fr.1C ($M_w = 1.70 \times 10^5$, $M_z/M_w = 1.23$, DS = 2.44), one of 12 fractions prepared previously[1] by the precipitation fractionation of commercial CDA (code CDA8, nominal DS = 2.34, DP = 180, Daicel Chem. Ind.) with mixed solvents of DMAc/methanol. The original CDA8 was produced from wood pulps by processes of acetylation (to cellulose triacetate, CTA) and ripening (hydrolysis of CTA to DS ≅ 2.34). For the fractionated sample Fr.1C, the individual degree of substitution at the C-2, 3, and 6 position hydroxyls of a glucose unit has recently been recharacterized by ^{13}C NMR measurements.[26] The result gave 0.85, 0.85, and 0.74 for the C-2, 3, and 6 position hydroxyls, respectively, and the total DS = 2.44. Higher content of OH groups was recognized at the C-6 position, which played the important role in the dynamics of the present system. The solvent, DMAc, was of high polarity and good solvent for CDA. It was purified by fractional column distillation under reduced pressure of N_2 atmosphere, the collected temperature being 70.5 °C at 21 mmHg.[1] The refractive index n_0 for the wavelength $\lambda_0 = 488$ nm was measured to be 1.4405 (Pulfrich refractometer, Shimadzu) and the viscosity η_s to be 0.838 cP at 30.0 °C.[1] Five semidilute solutions of $1.37c^*-4.90c^*$ were prepared by mixing the dried sample and solvent by weight and stayed for 1 week at 34 °C in a drybox with intermittent stirring. Here the overlapping polymer concentration c^* was determined from the relation $c^* = [\eta]^{-1} = 3.27 \times 10^{-3}$ g cm^{-3} with $[\eta]$ the intrinsic viscosity of Fr.1C in DMAc at 30.0 °C.[1] The polymer mass concentration c (g cm^{-3}) was determined by using the solvent density $\rho_s = 0.9323$ g cm^{-3} at 30.0 °C. The solution thus prepared was filtered through 0.20 μm pore-size filter (Sartorius) into the rinsed light scattering cell of 12 mm diameter and stored at 34 °C just prior to be served to measurements.

DLS Measurements and Data Reduction. DLS measurements were carried out by our laboratory-made software correlater of 512 channels (with equally spaced delay times)[27] and a multiple-tau digital correlator (ALV-5000/E with quasi-logarithmically spaced delay times) at 30.0 °C with the 488 nm line of an etalon-equipped argon ion laser (Spectra Physics 2020-03/2560, 3W). Our correlator counts the time interval between each two photons in a train of 1024 photons and repeats this process several times. In contrast to ALV-5000/E, which counts the number of photons in the gated interval, our correlator was absolutely effective in studying systems of weak scattered intensity.[27] The V_v component of the light scattered from the sample solution was measured in the range of the scattering angles θ of 10°−150° by the homodyne method[28] with the use of a laboratory-regulated photon counting unit of photomultiplier tube/amplifier/discriminator. Since no heterodyne feature was observed, the normalized scattered-intensity−time correlation function $g^{(2)}(t)$ was related to the electric-field time correlation function $g^{(1)}(t)$ by the Siegert relation. The $g^{(1)}(t)$ was analyzed satisfactorily by a sum of *single* exponentials, not a sum of stretched exponentials. Three methods of the histogram,[28,29] the inverse-Laplace transformation,[30] and the CONTIN methods[30] were used with the consistent results between them, where $g^{(1)}(t)$ was expressed by the relation $g^{(1)}(t) = \int G(\Gamma) \exp(-\Gamma t)\, d\Gamma$ with $G(\Gamma)$ the distribution function, or the fractional amplitude, of the decay rate Γ. $G(\Gamma)$ was reduced to three parts of discrete Γ-distribution as shown later. Each part was denoted as a type of motion i, and its dynamics was represented by the mean decay rate Γ_i and fractional amplitude f_i, which were averaged only over the ith distribution. If Γ_i is proportional to q^2, the relaxation process i is diffusion even in semidilute solution, and its behavior can be represented by the diffusion coefficient D_i.

Results and Discussion

The $g^{(2)}(t)$ Profile with Three Decay Modes. In Figure 2a, a typical example of the $g^{(2)}(t)$ data for CDA/DMAc in semidilute solution is shown by the $g^{(2)}(t)$ vs log(t) plot for $c = 4.90c^*$ at $\theta = 30°$ and $T = 30.0$ °C. The $g^{(2)}(t)$ curve is composed of three decay modes, which are represented in Figure 2b by the decay rate distribution $G(\Gamma)$ of three sharply separated peaks. The right side peak of largest Γ means the fast decay motion with the shortest correlation time $\tau = (2\Gamma)^{-1}$. We call it mode F (fast mode) and estimate the mean decay rate Γ_F by $\Gamma_F = \int_F \Gamma G(\Gamma)\, d\Gamma$, where the integration F is carried out only for the $G(\Gamma)$ corresponding to mode F. In the same way, we call tentatively the middle and the left-side peaks mode M (medium mode) and mode S (slow mode), respectively, and the corresponding mean decay rates Γ_M and Γ_S, respectively. In view of the analytical method of $g^{(1)}(t)$ where a simple exponential, not a stretched,

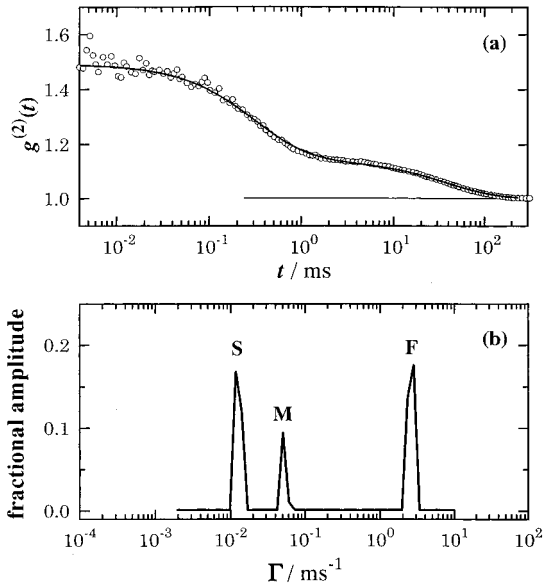

Figure 2. (a) $g^{(2)}(t)$ vs log t plot for the CDA/DMAc solution of $c = 4.90c^*$ at $\theta = 30°$. (b) Decay rate distribution analyzed by the inverse Laplace transformation for the $g^{(2)}(t)$ data.

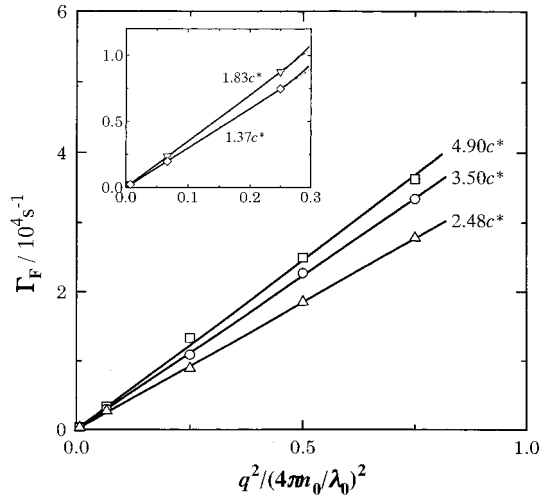

Figure 3. Scattering-vector dependence of the decay rate for fast mode Γ_F at five polymer mass concentrations of $1.37c^*-4.90c^*$.

decay form was used (see Experimental Section), the sharp $G(\Gamma)$ obtained for each mode implies the uniformity of relaxation time or size of motion.

Diffusive Nature of Three Modes. In Figure 3, the mean decay rate Γ_F at a given scattering vector $\boldsymbol{q}$ ($|\boldsymbol{q}| = q = (4\pi n_0/\lambda_0)\sin(\theta/2)$) and concentration c is plotted against $q^2/(4\pi n_0/\lambda_0)^2$ ($= \sin^2(\theta/2)$) for five solutions of $c = 1.37c^*-4.90c^*$. For each c at $c \geq 2.48c^*$, five data points at $\theta = 10°-120°$, or $\sin^2(\theta/2) = 0.0076-0.75$, are represented well by the straight line passing through the origin. For lower c of $1.37c^*$ and $1.83c^*$, the plot is given in the enlarged inset, where the linearity is obtained at $\theta \leq 60°$ or $\sin^2(\theta/2) \leq 0.25$ with a slightly upward deviation above $\theta > 60°$. Thus, mode F shows a diffusion motion, and the slope at $\theta \leq 60°$ gives the diffusion coefficient $D_F(c)$, defined by $D_F(c) = \Gamma_F(c)/q^2$, for each c. The same behavior was observed for other modes. Figure 4 shows the plot of $\Gamma_M(c)$ vs $q^2/(4\pi n_0/\lambda_0)^2$ for mode M. The linearity between $\Gamma_M(c)$ and q^2 is obtained for three higher c at $10° \leq \theta \leq 120°$ and two lower c at $10° \leq \theta \leq 60°$ (the enlarged inset). Therefore,

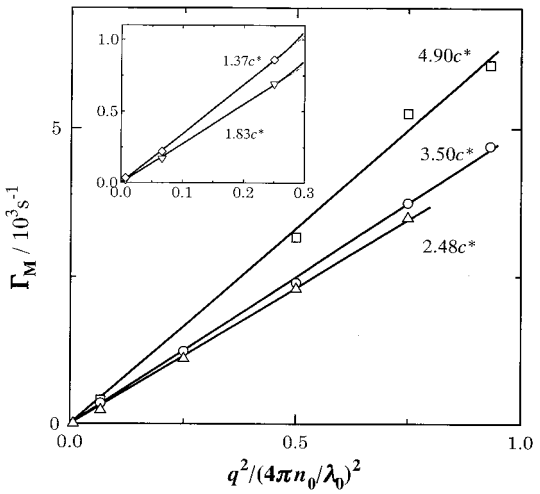

Figure 4. Scattering-vector dependence of the decay rate for medium mode Γ_M at five polymer mass concentrations of $1.37c^*-4.90c^*$.

this mode shows also another type of diffusive behavior. We obtained the diffusion coefficient $D_M(c)$ by $D_M(c) = \Gamma_M(c)/q^2$ from the straight lines. It is here noted that the upward deviations of data points from the straight lines, observed at higher θ in Figures 3 and 4, indicate that there are some local internal motions in modes F and M.[8] Figure 5a shows the q^2 dependence of $\Gamma_S(c)$ for mode S, where data for three higher c of $2.48c^*-4.90c^*$ are demonstrated. The data at $\theta = 10°-120°$ are all represented well by a straight line passing through the origin. These data, together with the data for lower c of $1.37c^*$ and $1.83c^*$, are plotted again in Figure 5b in the form of $\Gamma_S(c)/q^2$ vs q^2 plots. All data points for each c are constant over θ ranging from 10° to 120°. This fact certifies that the slow mode is exclusively a diffusion motion, no other motions being included. The diffusion coefficient at finite c, $D_S(c)$, was obtained by averaging the $\Gamma_S(c)/q^2$ values for each c.

Fast Mode as Cooperative Diffusion Motion. The diffusion coefficients $D_F(c)$, $D_M(c)$, and $D_S(c)$ thus estimated are plotted against the reduced concentration c/c^* in Figure 6 in the double-logarithmic scales, together with our previous data for CDA/DMAc in dilute solution (filled symbols) where three modes I, II, and III coexist.[2] The D_F data for fast mode (unfilled circles) are located roughly on the extended line from mode I, which represents the translational diffusion (the diffusion coefficient, D_G) of a single CDA molecule and the positive slope certifies the good solvent nature of the present CDA/DMAc system.[2] At $c > 1.83c^*$, however, D_F deviates clearly from D_G and increases with c/c^* with a larger slope than that for D_G. The dependence on concentration becomes

$$D_F(c) = 1.92 \times 10^{-6} c^{0.400}\ (\mathrm{cm^2\ s^{-1}})\ (\text{mode F}) \quad (1)$$

The correlation length ξ_F defined by

$$\xi_F(c) = k_B T/6\pi\eta_s D_F(c)\ (\text{mode F}) \quad (2)$$

is estimated to be 10−12 nm in the range of $c = 1.83c^*-4.90c^*$. This ξ_F value is much smaller than the radius of gyration $R_{G,0} \cong 40.2$ nm[31] estimated from the static LS data and is smaller than but comparable to the hydrodynamic Stokes radius $R_{H,0} = k_B T/6\pi\eta_s D_{G,c=0} = 16.3$ nm[1,2] of the present CDA chain at infinite dilution.

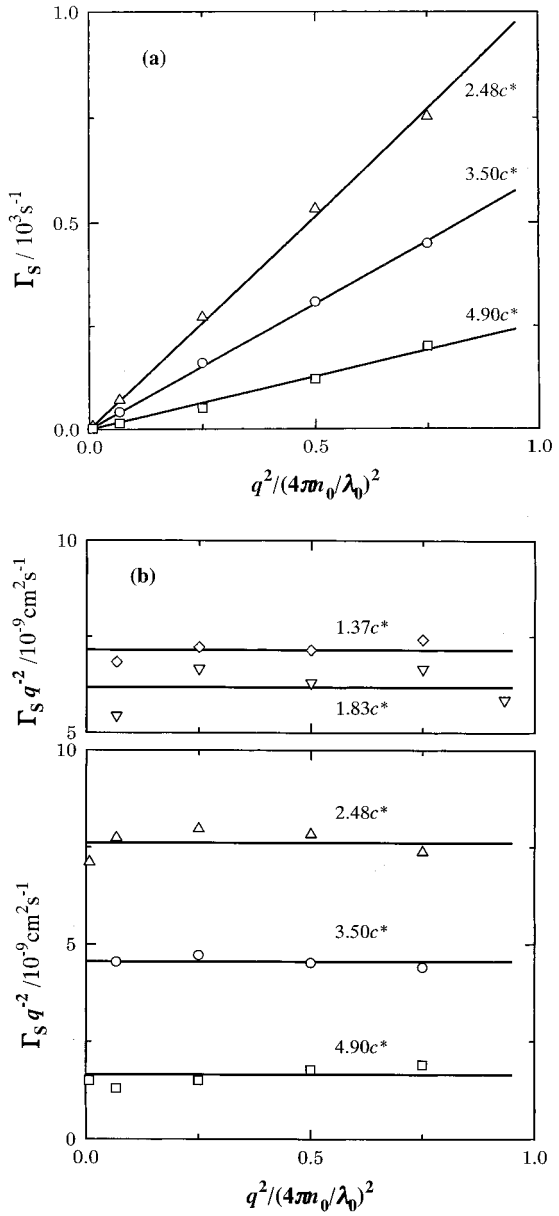

Figure 5. (a) Scattering-vector dependence of the decay rate for slow mode Γ_S at three polymer mass concentrations of $2.83c^*-4.90c^*$. (b) Γ_S/q^2 vs q^2 plots for five polymer mass concentrations of $1.37c^*-4.90c^*$. The constant value for each c represents the diffusion coefficient $D_S(c)$.

The CDA chain was less swollen by the hydrodynamic screening and by the screening of the excluded-volume interactions between monomers of the chain and induced the so-called temperature blobs (see below).[5,16]

For flexible linear polymers in good solvents, where no specific long-range interaction works, the fast mode motion appears in "the pseudogel domain" of semidilute solutions, which is defined in the qR_G-c/c^* diagram,[8] and emerges in the $D-c/c^*$ diagram as the extended line from the translational-diffusion mode in dilute solution. This mode is described as the cooperative diffusion, or the relaxation motions of concentration fluctuations, and can be expressed from the scaling argument[5] by

$$D_{coop} = D_0(c/c^*)^{\alpha}M^{0}, \quad \alpha = \nu/(3\nu - 1) \qquad (3)$$

Here ν is the excluded-volume exponents of $\nu = {}^3/_5$ and ${}^1/_2$ in the good- and Θ-solvent limits, respectively. For

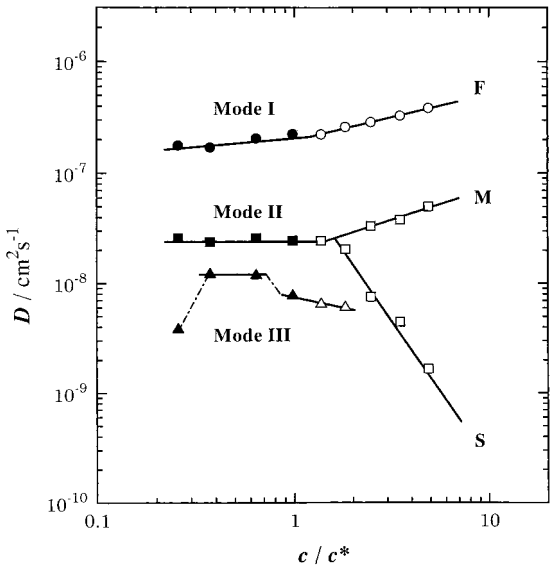

Figure 6. Concentration dependence of the diffusion coefficients D for fast (F), medium (M), and slow (S) modes in the semidilute solution region. Unfilled symbols represent the present data in semidilute solution and filled symbols our previous data in dilute solution.[1,2]

PS, the typical flexible chain, in good solvents the slope α was ranging from 0.4[8,9,11,16] to 0.67[7,10] or 0.72,[15] the latter larger values being still smaller than 0.75 or 0.77 predicted from the scaling theory[5] ($\nu = {}^3/_5$) or the renormalization group theory[32] ($\nu = 0.588$) in the good-solvent limit, though the correlation length ξ_F was independent of the molecular weight as predicted from the blob concept.[5] The smaller α cited above is explainable by assuming the marginal solvent region[16] between good- and Θ-solvent limits. In this region, a mean field situation holds and $\alpha = {}^1/_2$,[16] although it has not been clarified what is the motivation for occurring this situation. The difference between the larger α (=0.67−0.7) and the theoretical 0.75 would be improved by considering the effective (solution) viscosity[10] instead of the concentration-independent solvent viscosity that is assumed in the scaling argument for semidilute solution.

In view of the data connectivity between modes I and F in Figure 6, we ascribe mode F to the cooperative diffusion that represents the relaxation of concentration fluctuations in semidilute solution. Here many CDA chains can be divided into the concentration blobs of the size ξ_F, much smaller than that of freely expanded chain at infinite dilution, and their motions are not correlated to each other.[16] However, the exponent of concentration 0.40 in eq 1 is much smaller than the scaling value 0.75 for the semidilute solution in good solvents, not to speak of 1.0 for Θ solvents,[5] and rather resembles the experimental values of smaller α. That is, the present exponent is near ${}^1/_2$ predicted in marginal solvents for semidilute solutions[16] or in good solvents for the concentrated solution,[5] in both cases of which the concentration fluctuations can be treated by the Gaussian approximation or the random phase approximation, i.e., by the mean field theory.[4] Thus, the small exponent will lead to the following picture for mode F. In semidilute solution, the CDA/DMAc system is in the marginal solvent state, which is in contrast to the good solvent behavior in dilute solution.[2] The long-ranged intra- and intermolecular interactions which act between OH groups make the CDA cloud of ξ_F more tight than usual

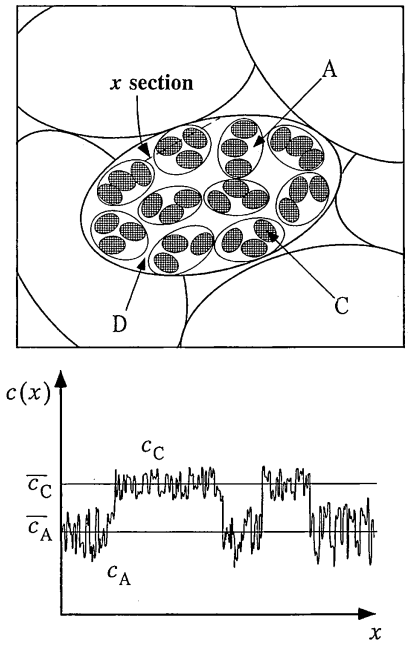

Figure 7. A nest of structures in dynamics for CDA in DMAc at $c > c^*$ (the upper part). The space C represents the concentration blob of the small correlation length ξ_F, the space being composed of the tightly packed CDA chain. The space A is another correlation blob of the correlation length ξ_M ($\cong 8\xi_F$), which represents a space of coarsely packed CDA chains. The space D is a time-space region where the blobs A are loosely packed with nonuniform distribution and the distribution fluctuates with time. In the lower part, the concentration fluctuation $c(x)$ in space C along a section x (a broken line) is plotted schematically against x. $\bar{c}_C$ and $\bar{c}_A$ are the mean values for the tentative values c_C and c_A in the spaces C and A, respectively.

chains and suppress the relaxation rates of concentration fluctuations (see Figure 7 and discussion later), which results in the mean field situation in the space of ξ_F. The small upward deviation of Γ_F at higher q in Figure 3 would indicate this situation: mode F includes a very small amount of local internal motions, which would be expected in "the internal motions domain" of the qR_G-c/c^* diagram in semidilute solution.[8]

Medium Mode as Cooperative Diffusion Motion. As shown by unfilled squares in Figure 6, the medium mode (called tentatively) shows unique behavior. At $c \geq 1.37c^*$, four unfilled squares of D_M data derive from mode II in dilute solution (the slope is slightly negative[2]) with a positive slope, 0.55, and gives the relation

$$D_M(c) = 4.56 \times 10^{-7} c^{0.548}\ (\mathrm{cm^2\ s^{-1}})\ (\text{mode M}) \quad (4)$$

Here, a data point at $c = 1.83c^*$, which is located below the fitted line of eq 4, was assigned to mode S, not to mode M, as described later. In the previous paper,[2] we have shown that mode II in dilute solution ($c < c^*$) represents the relaxation of concentration fluctuations, or the dissipation process, of "*the concentration clusters* created temporally and locally *within a limited small space in solution*" and that the clustering was originated from the hydrogen bond between CDA molecules via the polar solvent DMAc. In other words, mode II was the cooperative diffusion, not the translational diffusion of a larger associate of CDA molecules. This feature was rationalized by the viscosity behavior:[1] The intrinsic viscosity $[\eta]$ of CDA in DMAc revealed the exclusive presence of one kind of particle whose size was exactly the same as the single CDA molecule, no trace of association being detected. The concentration clusters created temporally in dilute solution will develop into substantial quasi-network structures at $c > c^*$. Mode M in semidilute solution can be thus assigned to the relaxation behavior of concentration fluctuations that are realized effectively within the quasi-network structures. Expressing its effective region by the correlation length $\xi_M(c) = k_B T/6\pi\eta_s D_M(c)$, we have the relation $\xi_M \cong 8\xi_F$ by comparing D_M and D_F data. This result indicates that modes M and F, both being the *cooperative diffusion*, construct in solution *a nest of structures* in the dynamic sense.[2] In other words, the CDA solution as a whole is never homogeneous but takes a hierarchy of dense-coarse concentrations in semidilute solution. The parallel, or a nonnested, dispersion of different structures in the solution would be disadvantageous to formation of *a limited number of structures of uniform size*, as are realized in Figure 2b by three sharply separated structures (see the previous section "The $g^{(2)}$-(t) Profile with Three Decay Modes").

A nest of structures is schematically given in the upper part of Figure 7. Several dense spaces C exist inside the less-dense space A, and a large number of spaces A are distributed inhomogeneously in a wider coarse space D. In the lower part of Figure 7, the scheme of concentration fluctuations $c(x)$ is presented along the section x in the space A. In the space C, the relaxation of concentration fluctuations is limited in the range smaller than a CDA chain size. This relaxation is very rapid because the concentration difference between the tentative concentration c_C and its mean $\bar{c}_C$, $|c_C - \bar{c}_C|$, is so small that the fluctuation of c_C relaxes quickly to the level of $\bar{c}_C$. The fluctuation then induces the cooperative diffusion of very fast decay (mode F), although it is effective only over the short length ξ_F. Meanwhile, the wider space A is considered to be composed of roughly packed CDA chains or several numbers of space C, as is indicated by $\xi_M \cong 8\xi_F$. The mean concentration $\bar{c}_A$ in the space A is lower than $\bar{c}_C$ in the space C, and the tentative fluctuation frequencies $|c_A - \bar{c}_A|$ are larger than $|c_C - \bar{c}_C|$ in the space C. Concentration fluctuations in the space A thus decay with the larger relaxation time or the smaller cooperative diffusion coefficient than that of mode F. We denote definitely these concentration fluctuations mode M and characterize it by D_M and ξ_M.

The concentration exponent 0.55 obtained in eq 4 for mode M is again smaller than the scaling value 0.75 but close to the experimentally obtained smaller values around 0.4 in good solvents or 0.5 in marginal solvents in semidilute solution of no specific long-range interactions. To the best of our knowledge, mode M is beyond example in the semidilute solution region. Only in the dilute solution region, a crude resemblance to our mode II and/or III has been observed on slow mode of starch fractions (the branched chains) in 0.5 N NaOH solution,[25] though the mode was assigned to the association due to branching and was retarded strongly in semidilute solution with $D \propto c^{-6.9}$. In the present case, CDA is the semiflexible linear chain of nearly monodispersed molecular weight, though heterogeneous in the sequence of C-2, 3, and 6 position OH groups along the chain contour.[1] The hydrogen-bond formation between C-6 position hydroxyls of different CDA molecules directly or via solvent DMAc is a key to accelerate the association[1] or the quasi-networks in semidilute solution. Moreover, the intramolecular hydrogen bond between

the C-3 position hydroxyls and the O-5′ position ring oxygens and/or between the C-2 position hydroxyls and the C-6′ position O-acetyls makes the chain stiffer.[1] Here the glucose units without prime (e.g., C-3) and with prime (e.g., O-5′) will be separated from each other by several or more glucose units along the chain contour. These long-range interactions will be more feasible in the overlapped chains and make quasi-network structures tight or less flexible. The marginal solvent situation would be again realized. However, the larger concentration exponent 0.55 of mode M than 0.40 of mode F would result from the looseness of quasi-network structures in the space A much more extreme than that in the space C. In this viewpoint, the small upward deviation of Γ_M observed at lower c ($=1.37-1.83c^*$) at higher q (Figure 4) is very suggestive because this result shows the presence of local internal motions in mode M.

Slow Mode and Self-Diffusion. The slow diffusion given in Figure 6 can be classified into two parts, one being mode III assigned in dilute solution (two unfilled triangles) and another being mode S really appeared in semidilute solution (four unfilled squares). At $c = 1.83c^*$, modes III and S coexist, but above $1.83c^*$ mode III disappears and mode S takes its place. In the previous paper,[2] mode III in dilute solution was assigned to the dissipation of a tentatively clustered dense CDA cloud to the level of bulk concentration. Since the solution is dilute, this cloud must be induced *inside* of another wider space of coarsely clustered CDA cloud, to this space we already referred as *a limited small space in solution* for mode II. A nest of structures are thus induced in dilute solution,[2] the former representing mode III and the latter (the outer coarse cloud, denoted as the space A_{pre}) mode II. However, when the bulk concentration c increases above c^*, the drastic change occurs in solution. The space A_{pre} becomes close to each other, and almost all the CDA are packed in A_{pre}, developing into the space A in Figure 7. In the beginning, the distribution of A will not be uniform over all the solution space, and the time-space fluctuation of this distribution (or the dense-coarse structure) will appear as a cooperative diffusion motion which could be represented by a huge space D with the correlation length ξ_{III}. This situation can be understood as two unfilled triangles in Figure 6. With more increase in c, the fluctuations in the space D will decrease and the uniform packing of blobs A will be achieved over the whole solution, as well as in D. Mode III will disappear in this stage. Then, mode S appears at c as high as $2c^*$ (see Figure 6), instead, where the uniform distribution of A could be realized in solution.

The diffusion coefficient, D_S, of mode S decreases sharply with c as shown in Figure 6. It gives the relation

$$D_S = 7.16 \times 10^{-14} c^{-2.44}\ (\mathrm{cm^2\ s^{-1}})\ (\text{mode S}) \quad (5)$$

The negative slope recalls the self-diffusion. However, the exponent -2.44, which was obtained in the range of $1.83c^*-4.90c^*$, is very large and is beyond $\beta = -1.75$ predicted as $D_{self} = D_0 \times (c/c^*)^{\beta} M^{-2}$ from the scaling theory in good solvents, $\beta = (\nu - 2)/(3\nu - 1)$ with $\nu = {}^3/_5$.[5] Experimentally, slow modes of motion have been reported in the semidilute region,[6−25] but only a few gave the extra-large exponents, that is, ca. -2 for PEO,[17] -2 or more for PMMA,[19] and -2.86 for CTC,[23] -2.56 for CT-3Cl-C,[24] and -1.85 and -6.9 for starch (branching through −O− bonds),[25] the last three of which are polysaccharides. Almost all of these slow motions have been discussed in terms of the transient clustering of loosely entangled chain or the movement of associates (clusters) through the solution strongly hindered.[17−19,23] It has also been observed that slow modes disappeared completely for covalently linked permanent networks,[11] and the slow diffusion coefficient was sometimes considerably smaller than the self-diffusion coefficients of pulsed field gradient NMR.[17] Thus, the movement of associates described above would be explained not by the real motion of the clusters through the transient network but by an apparent motion of clusters resulting from the random forming and breaking of network junctions.[25] Concerning only polysaccharides, we see that the β values of -2.86 and -2.56 for CTC[23] and CT-3Cl-C,[24] respectively, are close to ours. However, in these cases, all three hydroxyls in glucose residue on cellulose are substituted by the bulky groups of $OCO(NH)C_6H_5$ and $OCO(NH)C_6H_4Cl$ for CTC and CT-3Cl-C, respectively, no OH-groups remaining on the chain. The bulky side chains on the cellulose backbone hinder parallel stacking of the chains,[33] and rather make it easier to form entangled network, as large clusters were really recognized in the latter.[24] Thus, it would be conceivable for slow modes of CTC and CT-3Cl-C to be an apparent motion of clusters resulting from the random forming and breaking of transient network bonds. This situation would be different from that for the present CDA, where the nonbulky OH groups, as well as $OCOCH_3$ groups, sit on the cellulose backbone. Moreover, as was already discussed above on modes III and S, CDA was in densely packed state in the region where mode S appeared. Thus, it would follow that the present mode S may be a self-diffusion motion of a single CDA molecule, not an apparent motion of clusters. In this connection, it is very suggestive that α for fast mode was 0.9−1.0 for CTC and CT-3Cl-C, which was a striking contrast to 0.4 for the present CDA. It would be more conceivable for a single CDA to move through the solution strongly hindered. Many OH groups on the CDA chain are directly effective to formation of hydrogen bonds between other surrounding chains, which would make networks so tight that the random formation and breaking of bonds are suppressed. These networks would result in a virtual tube against a single CDA chain. The long-ranged hydrogen-bonding interaction between the single chain and the tube would retard the diffusion motion of the chain. In addition, the semiflexibility or the stiffness of CDA chain in DMAc[1] would depress the reptating diffusion all the more. Thus, mode S could be described by a reptating diffusion of the single CDA chain through the tube, the tube wall being composed of other surrounding CDA chains and possessing OH groups on the surface. During the reptation, the CDA chain would suffer the attractive long-range interaction from the tube wall.

Conclusion

The dynamics of cellulose derivative, or CDA, showed singular dynamic behavior in semidilute solution of polar solvents, DMAc. The dynamics would be specifically caused by the OH groups on the cellulose backbone. Thus, two cooperative diffusion motions and one self-diffusion motion realized were all retarded strongly by the long-ranged OH interactions (the hydrogen bond) which are affected between CDA chains directly or via polar solvents.

References and Notes

(1) Kawanishi, H.; Tsunashima, Y.; Okada, S.; Horii, F. *J. Chem. Phys.* **1998**, *108*, 6014.
(2) Kawanishi, H.; Tsunashima, Y.; Horii, F. *J. Chem. Phys.* **1998**, *109*, 11027.
(3) For example: (a) Tsunashima, Y.; Hirata, M.; Nemoto, N.; Kurata, M. *Macromolecules* **1987**, *20*, 1992. (b) Nemoto, N.; Makita, Y.; Tsunashima, Y.; Kurata, M. *Macromolecules* **1984**, *17*, 425.
(4) Doi, M.; Edwards, S. F. *The Theory of Polymer Dynamics*; Clarendon: Oxford, 1986.
(5) de Gennes, P. G. *Scaling Concepts in Polymer Physics*; Cornell University: Ithaca, NY, 1979.
(6) (a) Munch, J. P.; Candau, S.; Herz, J.; Hild, G. *J. Phys.* (*Paris*) **1977**, *38*, 971. (b) Munch, J. P.; Lemaréchal, P.; Candau, S.; Herz, J. *J. Phys.* (*Paris*) **1977**, *38*, 1499.
(7) (a) Adam, M.; Delsanti, M. *Macromolecules* **1977**, *10*, 1229. (b) Adam, M.; Delsanti, M.; Pouyet, G. *J. Phys. Lett.* (*Paris*) **1979**, *40*, L435.
(8) Chu, B.; Nose, T. *Macromolecules* **1980**, *13*, 122.
(9) Amis, E. J.; Han, C. C. *Polymer* **1982**, *23*, 1403.
(10) Nemoto, N.; Makita, Y.; Tsunashima, Y.; Kurata, M. *Macromolecules* **1984**, *17*, 2629.
(11) Candau, S. J.; Butler, I.; King, T. A. *Polymer* **1983**, *24*, 1601.
(12) Selser, J. C. *J. Chem. Phys.* **1983**, *79*, 1044.
(13) Amis, E. J.; Han, C. C.; Matsushita, Y. *Polymer* **1984**, *25*, 650.
(14) (a) Nemoto, N.; Inoue, T.; Makita, Y.; Tsunashima, Y.; Kurata, M. *Macromolecules* **1985**, *18*, 2516. (b) Nemoto, N.; Okada, S.; Inoue, T.; Tsunashima, Y.; Kurata, M. *Macromolecules* **1986**, *19*, 2305.
(15) Brown, W.; Nicolai, T. In *Dynamic Light Scattering*; Brown, W., Ed.; Clarendon: Oxford, 1993.
(16) Schaefer, D. W.; Han, C. C. In *Dynamic Light Scattering*; Pecora, R., Ed.; Prenum: New York, 1985.
(17) Brown, W. *Macromolecules* **1984**, *17*, 66.
(18) Eisele, M.; Burchard, W. *Macromolecules* **1984**, *17*, 1636; *Pure Appl. Chem.* **1984**, *56*, 1379.
(19) Ballodge, S.; Tirrell, M. *Macromolecules* **1985**, *18*, 819.
(20) Amis, E. J.; Janmey, P. A.; Ferry, J. F.; Yu, H. *Macromolecules* **1983**, *16*, 441.
(21) Herning, T.; Djabonrow, M.; Leblond, J.; Takerkart, G. *Polymer* **1991**, *32*, 3211.
(22) Mathiez, P.; Weisbuch, G. Mouttet, C. *Biopolymers* **1981**, *18*, 1465.
(23) Wenzel, M.; Burchard, W.; Schätzel, K. *Polymer* **1986**, *27*, 195.
(24) Klohr, E.; Zugenmaier, P. *Cellulose* **1994**, *1*, 259.
(25) Galinsky, G.; Burchard, W. *Macromolecules* **1996**, *29*, 1498.
(26) Hattori, K.; Tsunashima, Y.; Horii, F., to be published.
(27) Nemoto, N.; Tsunashima, Y.; Kurata, M. *Polym. J.* **1981**, *13*, 827.
(28) Tsunashima, Y.; Nemoto, N.; Kurata, M. *Macromolecules* **1983**, *16*, 584.
(29) Gulari, E.; Gulari, E.; Tsunashima, Y.; Chu, B. *J. Chem. Phys.* **1979**, *70*, 3965.
(30) Chu, B. *Laser Light Scattering*; Academic Press: New York, 1974 and 1991.
(31) (a) Kamide, K.; Saito, M. *Polym. J.* **1982**, *14*, 517. (b) Kamide, K.; Saito, M.; Abe, T. *Polym. J.* **1981**, *13*, 421.
(32) Le Guillou, J. C.; Zinn-Justin, J. *Phys. Rev. Lett.* **1977**, *39*, 95.
(33) Kimura, S. *Polym. Prepr. Jpn.* **1999**, *48*, 43.

MA9902145